TECHNICAL RESEARCH REPORT

Feedback Stabilization of PWM DC-DC Converters

by C.-C. Fang, E.H. Abed

T.R. 98-51

Feedback Stabilization of PWM DC-DC Converters

Chung-Chieh Fang and Eyad H. Abed
Department of Electrical Engineering
and Institute for Systems Research
University of Maryland
College Park, MD 20742 USA

Manuscript: September 28, 1998

Abstract

Feedback stabilization of the nominal periodic operating condition of PWM DC-DC converters is considered, using recently developed general sampled-data models. Two types of discrete-time washout filter aided feedback stabilization scheme are proposed and studied in detail. These are voltage reference compensation and dynamic ramp compensation. The stabilization schemes preserve the nominal periodic operating condition through washout filters as the system parameters vary.

1 Introduction

Pulse-width-modulated (PWM) DC-DC switching converters are widely used in industry and in consumer products. These converters are designed to operate in a stable fashion. However, in demanding applications they may be forced to operate in off-design conditions, in which case stability may be lost. An example of such a setting is a distributed power system where large disturbances might occur. The purpose of this paper is to develop new stabilization techniques for PWM DC-DC converters that can be used to ensure stability in an off-design condition. The new stabilization schemes are developed using general nonlinear sampled-data models recently developed by the authors [1, 2].

Two discrete-time washout filter aided stabilization schemes are proposed and developed in the paper: voltage reference compensation and dynamic ramp compensation. The nonlinear nature

of converter operation implies that the operating condition changes as parameters vary. Washout filters [3] are used in order to preserve the nominal operating branch.

Loss of stability in a nonlinear system generally coincides with the occurrence of a bifurcation of the nominal operating condition. Among the bifurcations found in PWM DC-DC converters are period-doubling bifurcation (subharmonic instability) [4, 5, 6, 7], saddle-node bifurcation [2], Neimark-Sacker bifurcation [2], border-collision bifurcation [8], and others [9]. This paper does not study these bifurcations in detail, but rather focuses on removing a bifurcation by stabilizing the branch in the parameter range of interest.

Several previous works have dealt with stabilization of the nominal periodic solution for a PWM DC-DC converter immediately following a bifurcation [10, 11, 12, 13]. In [10, 11, 12], targeting methods are used. In [13], a time-delay feedback method is used. The contribution of the present work lies in development of new stabilization schemes that are general and widely applicable. For the stabilization schemes proposed here, an added benefit is robustness in the sense that the nominal operating branch is preserved.

The remainder of the paper is organized as follows. In Section 2, a general model for PWM DC-DC converters developed by the authors in [1, 2] is reviewed. In Section 3, the two stabilization schemes proposed in this work are presented, namely voltage reference compensation and dynamic ramp compensation. In Section 4, two illustrative examples are given. Conclusions are collected in Section 5.

2 General Sampled-Data Model for PWM Converters

In this section, a summary of the sampled-data modeling of PWM converters discussed in [1, 2] is given. This includes a general block diagram model as well as associated nonlinear and linearized sampled-data models.

A block diagram model for a PWM converter in continuous conduction mode [14, pp. 165-168] is shown in Fig. 1. In the diagram, $A_1, A_2 \in \mathbf{R}^{N\times N}$, $B_1, B_2 \in \mathbf{R}^{N\times 1}$, $C, E_1, E_2 \in \mathbf{R}^{1\times N}$, and $D \in \mathbf{R}$ are constant matrices, $x \in \mathbf{R}^N$, $y \in \mathbf{R}$ are the state and the feedback signal, respectively, and N

is the state dimension, typically given by the number of energy storage elements in the converter. The source voltage is v_s, and the output voltage is v_o. The notation v_r denotes the reference signal, which could be a voltage or current reference. The reference signal v_r is allowed to be time-varying, although it is constant in most applications. The model in Fig. 1 is applicable both to voltage mode control [14, pp. 322-336] and current mode control [14, pp. 337-340]. The signal $h(t)$ is a T-periodic ramp. It is used to model a compensating ramp in current mode control. The clock has the same frequency $f_s = 1/T$ as the ramp. This frequency is called the switching frequency. Within a clock period, the dynamics is switched between the two stages S_1 and S_2. The system is in S_1 immediatedly following a clock pulse, and switches to S_2 at instants when $y(t) = h(t)$. Figure 2 illustrates the signal waveforms in the case of voltage mode control.

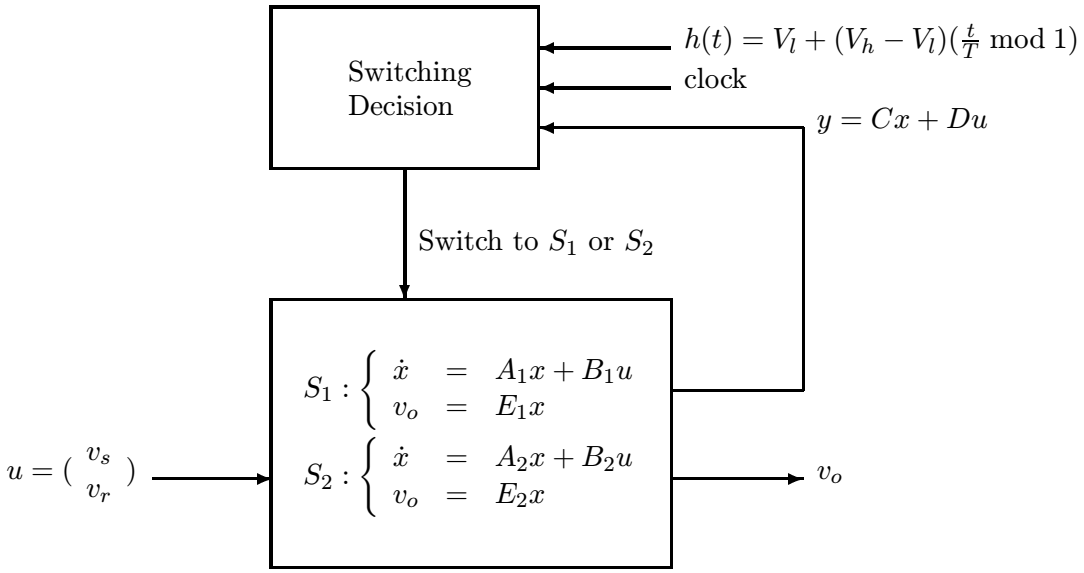

Figure 1: Block diagram model for PWM converter operation in continuous conduction mode

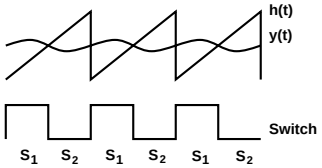

Figure 2: Waveforms for a PWM converter under voltage mode control

Consider the cycle $t \in [nT, (n+1)T)$. Take $u = (v_s, v_r)$ to be constant within the cycle, and denote its value by $u_n = (v_{sn}, v_{rn})$. Let $x_n = x(nT)$ and $v_{on} = v_o(nT)$. Denote by $nT + d_n$ the switching instant within the cycle when $y(t)$ and $h(t)$ intersect. Then, the system in Fig. 1 has the following sampled-data dynamics:

$$\begin{aligned} x_{n+1} &= f(x_n, u_n, d_n) \\ &= e^{A_2(T-d_n)}(e^{A_1 d_n} x_n + \int_0^{d_n} e^{A_1(d_n-\sigma)} d\sigma B_1 u_n) + \int_{d_n}^{T} e^{A_2(T-\sigma)} d\sigma B_2 u_n \qquad (1) \\ g(x_n, u_n, d_n) &= C(e^{A_1 d_n} x_n + \int_0^{d_n} e^{A_1(d_n-\sigma)} d\sigma B_1 u_n) + D u_n - h(d_n) \\ &= 0 \qquad (2) \end{aligned}$$

A periodic solution $x^0(t)$ in Fig. 1 corresponds to a point $x^0(0)$ in the sampled data dynamics (1), (2. Let the fixed point of the system (1), (2) be $(x_n, u_n, d_n) = (x_n, [v_{sn}, v_{rn}]', d_n) = (x^0(0), [V_s, V_r]', d)$. Using a hat $\hat{}$ to denote small perturbations (e.g., $\hat{x}_n = x_n - x^0(0)$), the system (1), (2) has the linearized dynamics

$$\hat{x}_{n+1} = \Phi \hat{x}_n + \Gamma \hat{u}_n = \Phi \hat{x}_n + \Gamma_1 \hat{v}_{sn} + \Gamma_2 \hat{v}_{rn} \qquad (3)$$

where

$$\begin{aligned} \Phi &= e^{A_2(T-d)}(I - \frac{((A_1 - A_2)x^0(d) + (B_1 - B_2)u)C}{C(A_1 x^0(d) + B_1 u) - \dot{h}(d)}) e^{A_1 d} \\ &= e^{A_2(T-d)}(I - \frac{(\dot{x}^0(d^-) - \dot{x}^0(d^+))C}{C\dot{x}^0(d^-) - \dot{h}(d)}) e^{A_1 d} \qquad (4) \\ \Gamma &= e^{A_2(T-d)}(\int_0^d e^{A_1\sigma} d\sigma B_1 - \frac{\dot{x}^0(d^-) - \dot{x}^0(d^+)}{C\dot{x}^0(d^-) - \dot{h}(d)}(C \int_0^d e^{A_1\sigma} d\sigma B_1 + D)) + \int_0^{T-d} e^{A_2\sigma} d\sigma B_2 \qquad (5) \end{aligned}$$

3 Discrete-Time Washout Filter Aided Stabilization Schemes

There may exist unstable periodic orbits (UPOs) with different periods when the PWM converter is unstable. Here we only show stabilization of the nominal T-periodic UPO. A similar approach

can be applied to stablize a general nT-periodic UPO. We will show this through an example (for n=2) in Sec. 4.

From Fig. 1, feedback stabilization can be achieved by adjusting v_s, v_r, and $h(t)$ (or equivalently y). Generally v_s undergoes large variations and is therefore not a candidate as a control variable. In this section, feedback stabilization is achieved by adjusting v_r or $h(t)$.

3.1 Washout Filter Aided Voltage Reference (v_r) Compensation

In the first stabilization scheme, v_r is updated at the clock time. Denote it as $v_{rn} = V_r + \hat{v}_{rn}$, where V_r is the nominal voltage reference value. The system diagram is shown in Fig. 3. The proposed washout filter aided discrete-time controller is

$$w_{n+1} = -K_1 x_n + (1 - K_2) w_n \tag{6}$$

$$\hat{v}_{rn} = -K_1 x_n - K_2 w_n \tag{7}$$

where $w_n \in \mathbf{R}$ is the state of the washout filter, $K_1 \in \mathbf{R}^{1\times N}$, $K_2 \in \mathbf{R}$ are the feedback gains and $K_2 \neq 0$. In steady state, $\hat{v}_{rn}$=0. Thus the original fixed point $x_n = x^0(0)$ in the system (1), (2) is preserved.

The closed-loop system (1), (2), (6), (7) has the following linearized dynamics

$$\begin{bmatrix} \hat{x}_{n+1} \\ \hat{w}_{n+1} \end{bmatrix} = \left(\begin{bmatrix} \Phi & 0 \\ 0 & 1 \end{bmatrix} - \begin{bmatrix} \Gamma_2 \\ 1 \end{bmatrix} \begin{bmatrix} K_1 & K_2 \end{bmatrix} \right) \begin{bmatrix} \hat{x}_n \\ \hat{w}_n \end{bmatrix} \tag{8}$$

One has the following result.

Theorem 1 *The nominal fixed point of system (1), (2) is asymptotically stabilizable by the washout filter aided voltage reference control scheme if the following conditions are satisfied:*

(i) (Φ, Γ_2) *is stabilizable.*

(ii) $\begin{bmatrix} \Phi - I & \Gamma_2 \\ 0 & 1 \end{bmatrix}$ *is of full rank.*

Proof:

If condition (ii) holds, then the eigenvalue at 1 (introduced by the washout filter) is controllable,

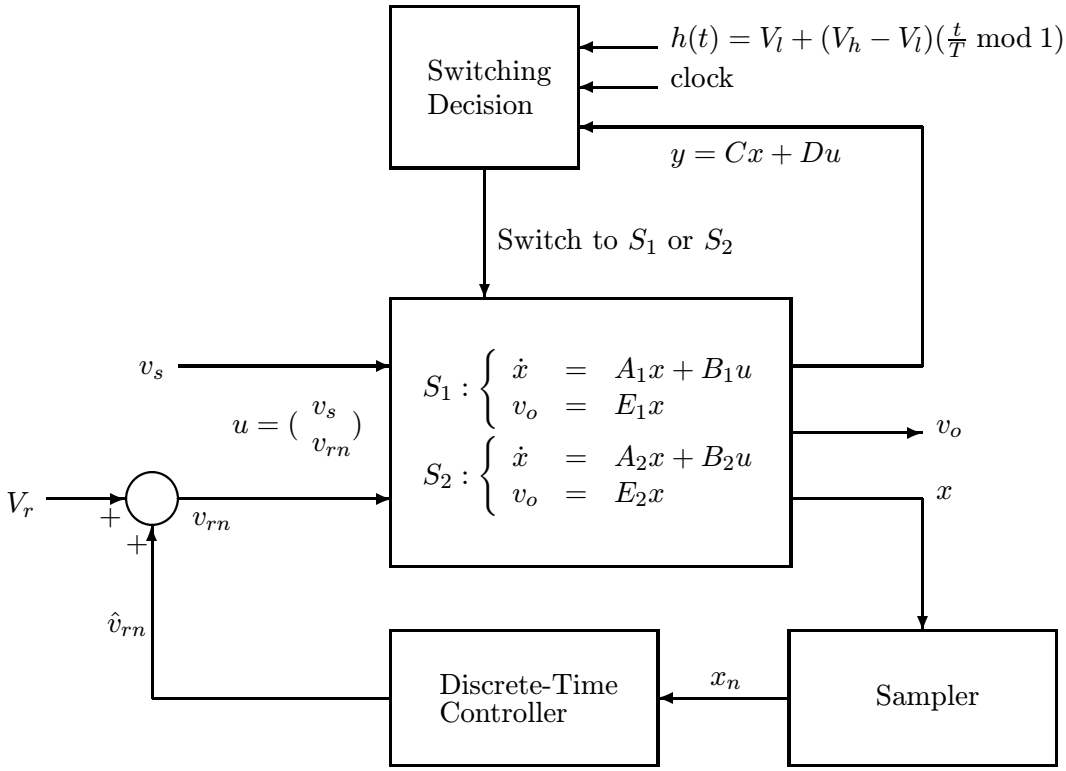

Figure 3: Stabilization by voltage reference (v_r) compensation

by the PBH rank test [15]. Let λ be any eigenvalue of Φ which lies outside the unit circle. This eigenvalue is controllable if $\begin{bmatrix} \Phi - \lambda I & 0 & \Gamma_2 \\ 0 & 1-\lambda & 1 \end{bmatrix}$ is of full rank. This matrix is of full rank if condition (i) holds. □

3.2 Washout Filter Aided Dynamic Ramp Compensation

Next, a scheme is presented in which the slope of the ramp $h(t)$ is changed by state feedback. The signal $h(t)$ is called a *dynamic ramp*, to distinguish it from the traditional fixed-slope compensating ramp. The system diagram is shown in Fig. 4. The proposed discrete-time controller is

$$w_{n+1} = -K_1x_n + (1 - K_2)w_n \tag{9}$$

$$\hat{v}_{hn} = -K_1x_n - K_2w_n \tag{10}$$

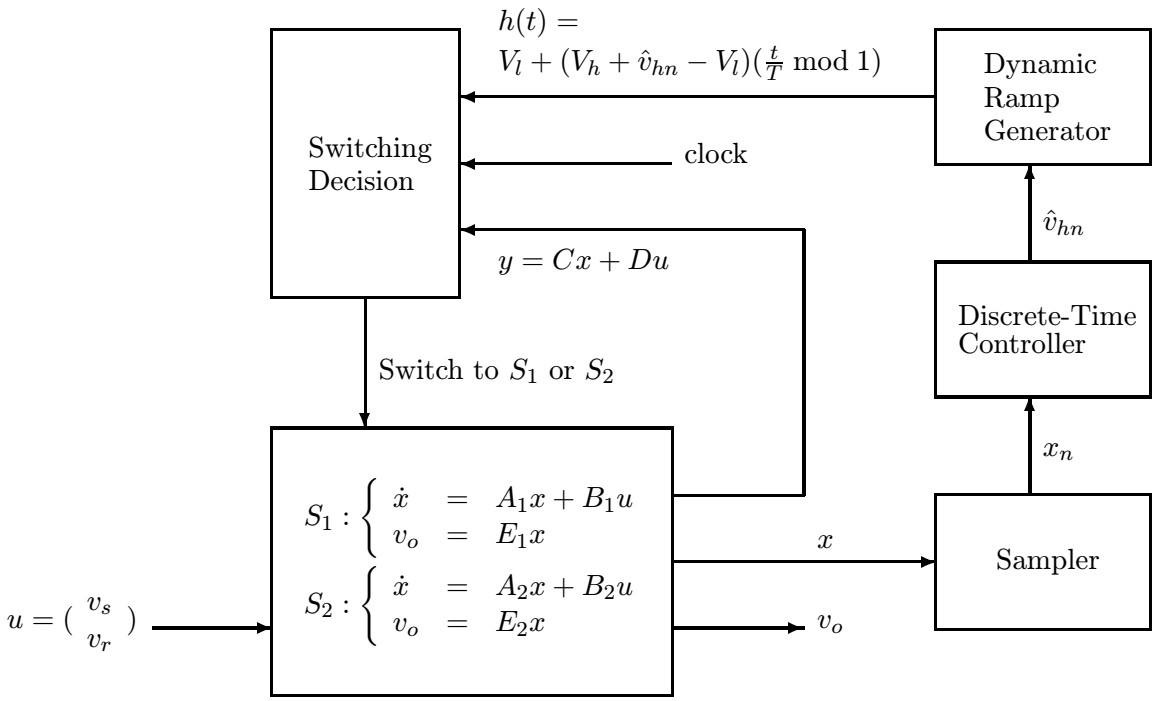

Figure 4: Stabilization by dynamic ramp compensation

where $w_n \in \mathbf{R}$ is the state of the washout filter, $K_1 \in \mathbf{R}^{1\times N}$, $K_2 \in \mathbf{R}$ are the feedback gains and $K_2 \neq 0$. As was the case with the washout filter aided voltage reference compensation, the original fixed point $x_n = x^0(0)$ in the system (1), (2) is preserved.

Let $h(t) = V_l + (v_h - V_l)(\frac{t}{T} \bmod 1)$. Changing the slope is equivalent to changing v_h. Let v_h be updated in each cycle and denoted as $v_{hn} = V_h + \hat{v}_{hn}$, where V_h is constant. The switching constraint equation, Eq. (2), now becomes

$$\begin{aligned} g(x_n, u_n, d_n, v_{hn}) &= C(e^{A_1 d_n} x_n + \int_0^{d_n} e^{A_1(d_n-\sigma)} d\sigma B_1 u_n) + Du_n - V_l - \frac{(v_{hn} - V_l)d_n}{T} \\ &= 0 \end{aligned} \tag{11}$$

The closed-loop system (1), (11), (9), (10) has the linearized dynamics

$$\begin{bmatrix} \hat{x}_{n+1} \\ \hat{w}_{n+1} \end{bmatrix} = (\begin{bmatrix} \Phi & 0 \\ 0 & 1 \end{bmatrix} - \begin{bmatrix} \Gamma_h \\ 1 \end{bmatrix} \begin{bmatrix} K_1 & K_2 \end{bmatrix}) \begin{bmatrix} \hat{x}_n \\ \hat{w}_n \end{bmatrix} \tag{12}$$

where

$$\Phi = \frac{\partial f}{\partial x_n} - \frac{\partial f}{\partial d_n}(\frac{\partial g}{\partial d_n})^{-1}\frac{\partial g}{\partial x_n}\Big|_{(x_n,u_n,d_n,v_{hn})=(x^0(0),u,d,V_h)}$$

$$= e^{A_2(T-d)}(I - \frac{(\dot{x}^0(d^-) - \dot{x}^0(d^+))C}{C\dot{x}^0(d^-) - \frac{V_h - V_l}{T}})e^{A_1 d} \tag{13}$$

$$\Gamma_h = -\frac{\partial f}{\partial d_n}(\frac{\partial g}{\partial d_n})^{-1}\frac{\partial g}{\partial v_{hn}}\Big|_{(x_n,u_n,d_n,v_{hn})=(x^0(0),u,d,V_h)}$$

$$= e^{A_2(T-d)}\frac{(\dot{x}^0(d^-) - \dot{x}^0(d^+))d}{(C\dot{x}^0(d^-) - \frac{V_h - V_l}{T})T} \tag{14}$$

Analogous to Theorem 1, one has

Theorem 2 *Assume that A_1 and A_2 have no eigenvalues with positive real part, and that at least one of these matrices have all eigenvalues with negative real part. If the matrix* $\begin{bmatrix} \Phi - I & \Gamma_h \\ 0 & 1 \end{bmatrix}$ *is of full rank, the system (1), (2) is asymptotically stabilizable using the washout filter aided dynamic ramp scheme.*

Proof:

Let $K_1 = -\frac{T}{d}Ce^{A_1 d}$, then $\Phi - \Gamma_h K_1 = e^{A_2(T-d)}e^{A_1 d}$, the eigenvalues of which lie inside the unit circle by Proposition A.1 in Appendix A. Thus the pair (Φ, Γ_h) is asymptotically stabilizable. The rest of the proof is similar to that of Theorem 1. □

4 Illustrative Examples

Example 1. (*Discrete-time stabilization of a buck converter under voltage mode control*) Consider the buck converter under voltage mode control shown in Fig. 5. Let $T = 400\mu s$, $L = 20mH$, $C = 47\mu F$, $R = 22\Omega$, $V_r = 11.3V$, $g_1 = 8.4$, $V_l = 3.8V$, $V_h = 8.2V$ implying $h(t) = 3.8 + 4.4[\frac{t}{T} \bmod 1]$, and let V_s be the bifurcation parameter. For this circuit, N=2 and the matrices in the model of

Fig. 1 with state $x = (i_L, v_C)$ are given by [2]

$$
\begin{aligned}
A_1 &= A_2 = \begin{bmatrix} 0 & \frac{-1}{L} \\ \frac{1}{C} & \frac{-1}{RC} \end{bmatrix} \\
B_1 &= \begin{bmatrix} 0 \\ 0 \end{bmatrix} \qquad\qquad B_2 = \begin{bmatrix} \frac{1}{L} \\ 0 \end{bmatrix} \\
C &= \begin{bmatrix} 0 & g_1 \end{bmatrix} \qquad\qquad D = \begin{bmatrix} 0 & -g_1 \end{bmatrix} \\
E_1 &= E_2 = \begin{bmatrix} 0 & 1 \end{bmatrix}
\end{aligned}
$$

The bifurcation diagram for the circuit is shown in Fig. 6. The circuit is chaotic for $V_s = 34.66V$. Here stabilization of this system is demonstrated by using washout filter aided voltage reference or dynamic ramp compensation.

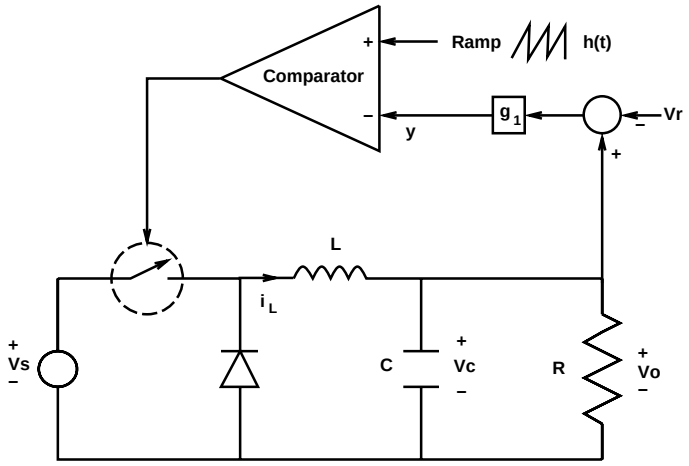

Figure 5: System diagram for Example 1

The pairs $(\begin{bmatrix} \Phi & 0 \\ 0 & 1 \end{bmatrix}, \begin{bmatrix} \Gamma_2 \\ 1 \end{bmatrix})$ (Eq. (8)) and $(\begin{bmatrix} \Phi & 0 \\ 0 & 1 \end{bmatrix}, \begin{bmatrix} \Gamma_h \\ 1 \end{bmatrix})$ (Eq. (12)) for this example can be shown to be controllable, so all of the eigenvalues of the closed-loop system can be assigned to the origin. In an N-dimensional linear time-invariant discrete system, assigning all of the poles of the closed-loop system to zero is called dead-beat control. This is because with such a control law, the system is driven to the origin in finitely many (N) steps. In the switching converter, the dynamics is nonlinear, so the dead-beat effect cannot be guaranteed to occur, but fast stabilization is expected if a linear dead-beat control is used.

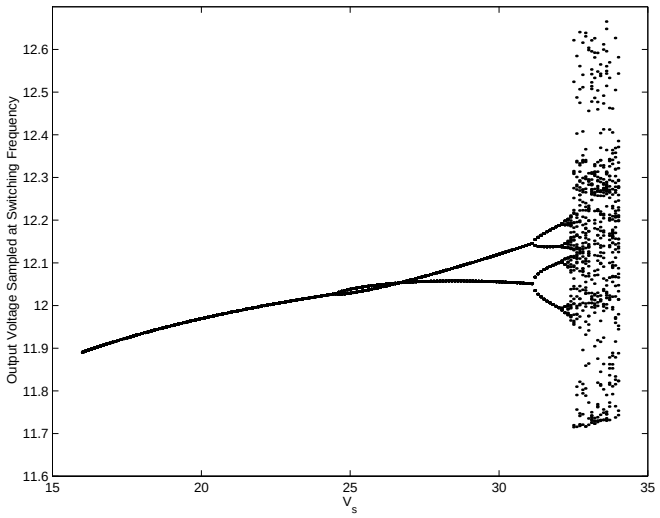

Figure 6: Bifurcation diagram for the circuit in Fig. 5

First, use v_r as the control variable and assign all of the closed-loop eigenvalues to 0. The feedback gains achieving this are $K_1 = (-1.6622, -0.4655)$ and $K_2 = 0.2403$. Fig. 7 shows the effectiveness of the control law. Originally the system is chaotic. When the control scheme is applied at $t = 0.0048$, the chaotic trajectory is stabilized to a period-one orbit in around 3 switching periods. The stabilized period-one orbit is shown in Fig. 8.

Next, dynamic ramp control is applied. The effectiveness of washout filter aided dynamic ramp compensation in stabilizing the UPO is illustrated in Fig. 9. The feedback gains used in this illustration are $K_1 = (-21.4809, -6.0160)$ and $K_2 = 0.2403$, which also makes all of the closed-loop eigenvalues at 0. Similar to the result of using v_r as control variable, the periodic solution is stabilized in around three switching periods. Fig. 10 shows the bifurcation diagram with the same feedback gains. The stable operating range is now extended up to a source voltage of $V_s = 35V$.

In this example, a chaotic system is stabilized by simple state feedback, which can be compared, for instance, with the complicated algorithm proposed in [11].

Generally switching converters are designed to operate in the period-*one* mode, not in any higher periodic mode. It is known that in a chaotic system there are an infinite number of *unstable* periodic solutions embedded in the chaotic orbit. To show the flexibility of the control methods

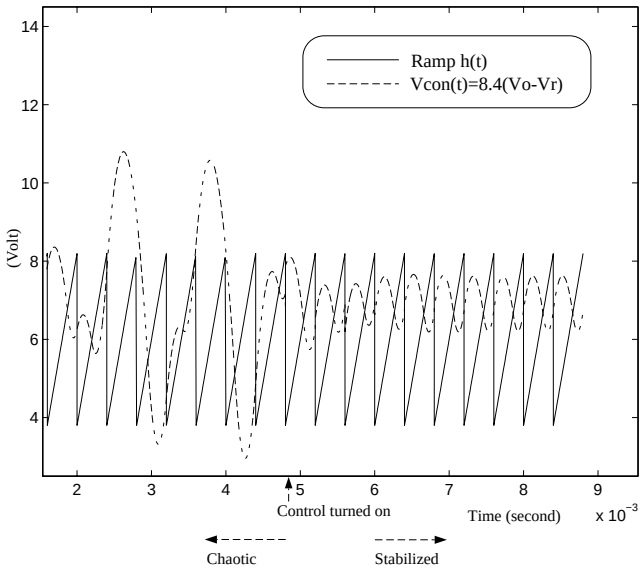

Figure 7: Stabilization of the buck converter in Fig. 5 using washout filter aided voltage reference compensation; control turned on at $t = 0.0048$

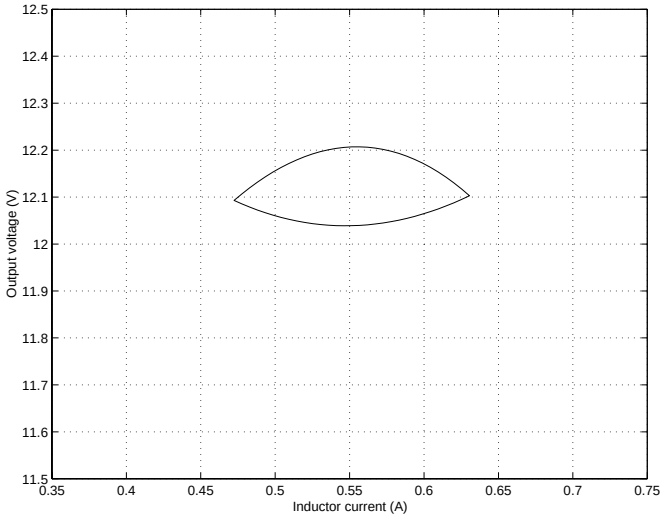

Figure 8: Stabilized period-one orbit in state space for $V_s = 34.66V$

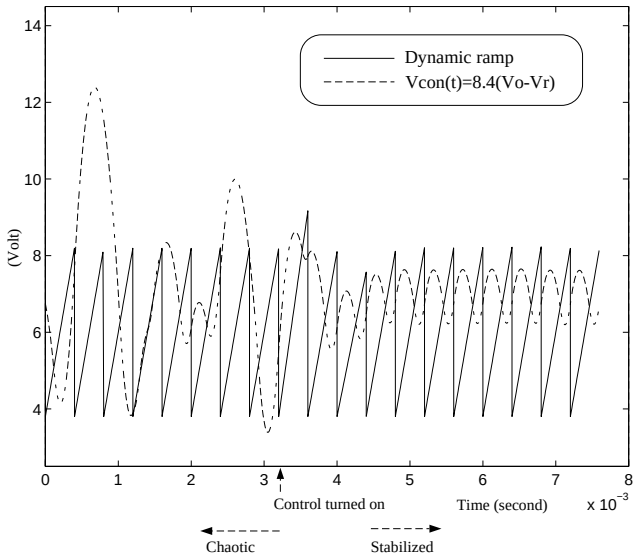

Figure 9: Stabilization of the buck converter in Fig. 5 using washout filter aided dynamic ramp compensation; control turned on at $t = 0.0032$

presented in the paper, stabilization of a period-two orbit is demonstrated next.

Similar to stabilization of the period-one mode, the period-two dynamics can be derived and linearized. Washout filter aided voltage reference compensation is used. All of the closed-loop poles are assigned to zero using feedback gains $K_1 = (0.006616, -0.59)$ and $K_2 = 0.23426$. The sampling rate for feedback stabilization in this case is *half* of the switching frequency. A simulation showing stabilization of the period-two orbit is given in Fig. 11, and the stabilized period-two orbit is shown in Fig. 12.

Example 2 (*Discrete-time stabilization of a boost converter under current mode control*) Consider the boost converter under current mode control shown in Fig. 13, where $T = 100\mu s$, $V_s = 10V$, $L = 1mH$, $C = 12\mu F$, $R = 20\Omega$, and V_r (current reference) is taken to be the bifurcation parameter. For this circuit, N=2 and the matrices in the model of Fig. 1 with state $x = (i_L, v_C)$ are given

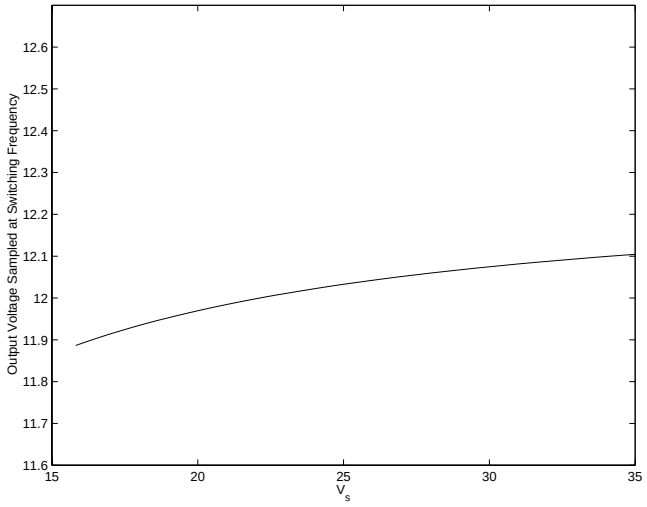

Figure 10: Bifurcation diagram for Example 1 using washout filter aided dynamic ramp compensation

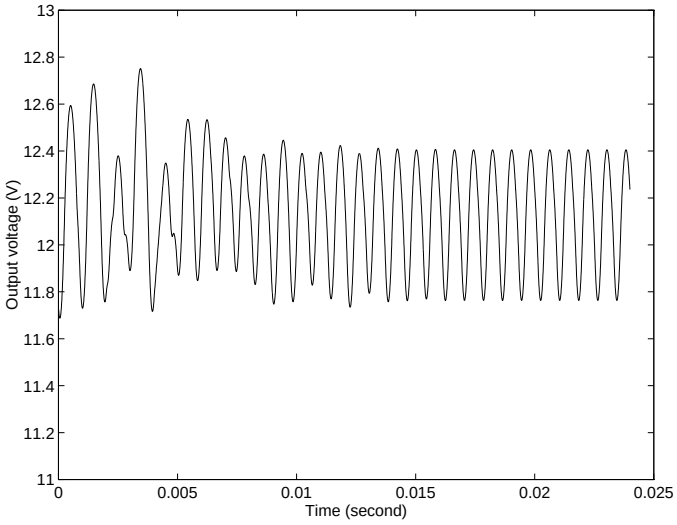

Figure 11: Stabilization of period-two orbit; control turned on at $t = 4.8 \times 10^{-3}$

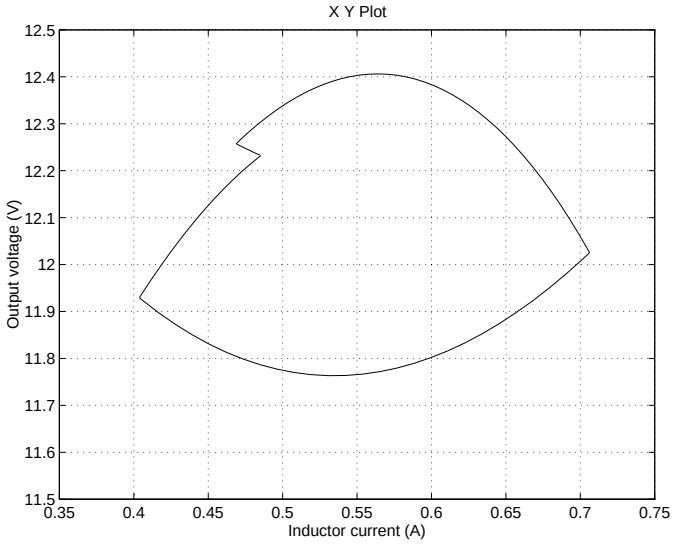

Figure 12: Stabilized period-two orbit in state space for $V_s = 34.66V$

by [2]

$$A_1 = \begin{bmatrix} 0 & 0 \\ 0 & \frac{-1}{RC} \end{bmatrix} \qquad A_2 = \begin{bmatrix} 0 & \frac{-1}{L} \\ \frac{1}{C} & \frac{-1}{RC} \end{bmatrix} \qquad B_1 = B_2 = \begin{bmatrix} \frac{1}{L} \\ 0 \end{bmatrix}$$
$$C = \begin{bmatrix} 1 & 0 \end{bmatrix} \qquad D = \begin{bmatrix} 0 & -1 \end{bmatrix} \qquad E_1 = E_2 = \begin{bmatrix} 0 & 1 \end{bmatrix}$$

The bifurcation diagram for the circuit is shown in Fig. 14. The circuit is in period-two mode for $V_r = 1.85$. Here stabilization of the nominal period-one mode using washout filter aided dynamic ramp compensation for $V_r = 1.85$ will be demonstrated.

It can be checked that the pair $(\begin{bmatrix} \Phi & 0 \\ 0 & 1 \end{bmatrix}, \begin{bmatrix} \Gamma_h \\ 1 \end{bmatrix})$ is controllable for this example. Therefore the closed-loop eigenvalues can be placed so as to achieve dead-beat control (similar to the approach in the preceding example).

Using dynamic ramp compensation, the period-one mode can be stabilized (in around three switching periods) so that it replaces the period-two mode as shown in Fig. 15.

If stabilization of a wide range of V_r values is desired, Ackermann's formula [15] can be used to schedule the gain. The resulting bifurcation diagram is shown in Fig. 16.

The performance has been compared with traditional fixed-slope compensation with a slope of

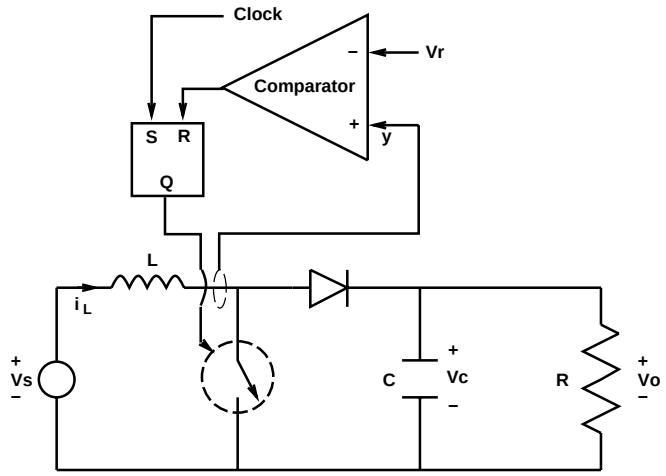

Figure 13: System diagram for Example 2

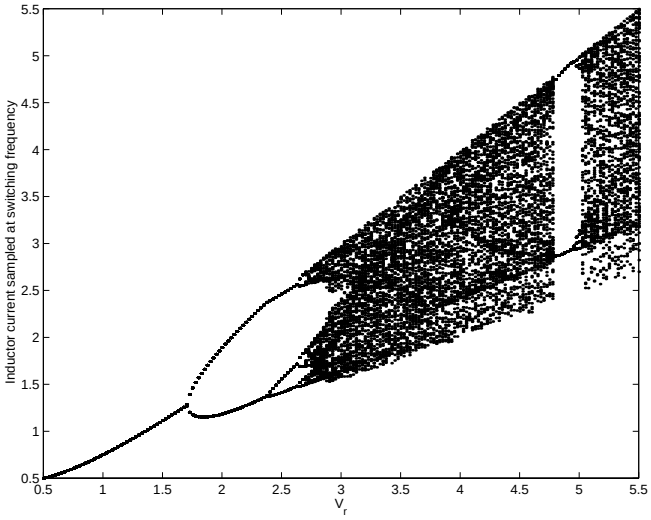

Figure 14: Bifurcation diagram for the circuit in Fig. 13

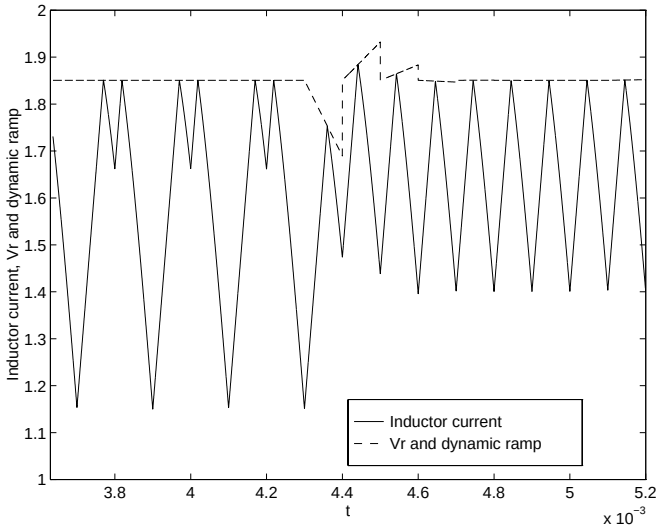

Figure 15: Stabilization of the boost converter in Fig. 13 using washout filter aided dynamic ramp compensation; control turned on at $t = 4.3 \times 10^{-3}$

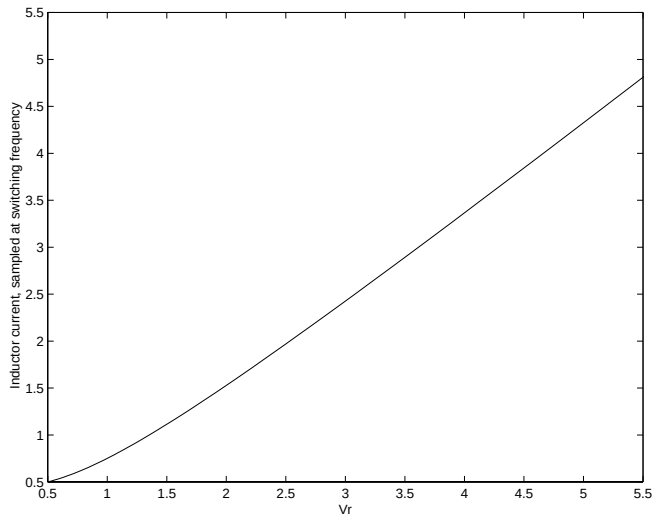

Figure 16: Bifurcation diagram for Example 3 using dynamic ramp compensation and gain scheduling

value 10000 *Amp/sec*. A delay in the period-doubling bifurcation was achieved, at the expense of altering the nominal operating branch. Details are in [2].

5 Concluding Remarks

Feedback stabilization of the nominal periodic orbit in the PWM DC-DC converter has been studied. Two schemes were proposed: voltage reference compensation and dynamic ramp compensation, both implemented through a washout filter. The same schemes can be used to stabilize an unstable period-two orbit or a higher order orbit. Washout filters ensure that the nominal operating branch is unaffected by the control, without the need for accurate knowledge of the equilibrium. Conditions for stabilizability have been derived. The proposed stabilization schemes are simple and systematic.

Acknowledgments

This research has been supported in part by the the Office of Naval Research under Multidisciplinary University Research Initiative (MURI) Grant N00014-96-1-1123, the U.S. Air Force Office of Scientific Research under Grant F49620-96-1-0161, and by a Senior Fulbright Scholar Award.

References

[1] C.-C. Fang and E.H. Abed, "Sampled-data modeling and analysis of PWM DC-DC converters I. Closed-loop circuits," preprint, Feb. 1998.

[2] C.-C. Fang, *Sampled-Data Analysis and Control of DC-DC Switching Converters*, Ph.D. thesis, University of Maryland, College Park, 1997.

[3] E.H. Abed, H.O. Wang, and R.C. Chen, "Stabilization of period doubling bifurcations and implications for control of chaos," *Physica D*, vol. 70, no. 1-2, pp. 154–164, 1994.

[4] J.H.B. Deane and D.C. Hamill, "Instability, subharmonics, and chaos in power electronics circuits," *IEEE Transactions on Power Electronics*, vol. 5, no. 3, pp. 260–268, 1990.

[5] D.C. Hamill, J.H.B. Deane, and J. Jefferies, "Modeling of chaotic DC-DC converters by iterated nonlinear mappings," *IEEE Transactions on Power Electronics*, vol. 7, no. 1, pp. 25–36, 1992.

[6] J.H.B. Deane, "Chaos in a current-mode controlled boost DC-DC converter," *IEEE Transactions on Circuits and Systems-I: Fundamental Theory and Applications*, vol. 39, no. 8, pp. 680–683, 1992.

[7] C.K. Tse, "Flip bifurcation and chaos in three-state boost switching regulators," *IEEE Transactions on Circuits and Systems-I: Fundamental Theory and Applications*, vol. 41, no. 1, pp. 16–23, 1994.

[8] S. Banerjee, E. Ott, J. A. Yorke, and G. H. Yuan, "Anomalous bifurcations in DC-DC converters: Borderline collisions in piecewise smooth maps," in *IEEE Power Electronics Specialists Conf. Rec.*, 1997, pp. 1337–1344.

[9] P.T. Krein and R.M. Bass, "Types of instability encountered in simple power electronic circuits: unboundedness, chattering, and chaos," in *Fifth Annual Applied Power Electronics Conference and Exposition*, 1990, pp. 191–194.

[10] G. Podder, K. Chakrabarty, and S. Banerjee, "Control of chaos in the boost converter," *Electronics Letters (IEE)*, vol. 31, no. 11, pp. 25, 1995.

[11] G. Podder, K. Chakrabarty, and S. Banerjee, "Experimental control of chaotic behavior of buck converter," *IEEE Transactions on Circuits and Systems-I: Fundamental Theory and Applications*, vol. 42, no. 8, pp. 100–101, 1995.

[12] P.J. Aston, J.H.B. Deane, and D.C. Hamill, "Targeting in systems with discontinuities, with applications to power electronics," *IEEE Transactions on Circuits and Systems-I: Fundamental Theory and Applications*, vol. 44, no. 10, pp. 1034–1039, 1997.

[13] C. Batlle, E. Fossas, and G. Olivar, "Time-delay stabilization of the buck converter," in *International Conference, Control of Oscillations and Chaos Proceedings*, 1997, vol. 3, pp. 590–593.

[14] N. Mohan, T.M. Undeland, and W.P. Robbins, *Power Electronics: Converters, Applications, and Design*, Wiley, New York, 1995.

[15] T. Kailath, *Linear Systems*, Prentice-Hall, Englewood Cliffs, NJ., 1980.

A A Stability Lemma

Generally the converter will dissipate energy due to the inherent resistance, so all of the eigenvalues of A_1 and A_2 are in the open left half of the complex plane. (None can be in the right half of the complex plane since the circuit is a single RLC circuit between switching instants.) If some of the resistances in the circuit are not modeled, then A_1 or A_2 may have some eigenvalues on the imaginary axis. Assume $\mathrm{Re}[\sigma(A_1)] \leq 0$ and $\mathrm{Re}[\sigma(A_2)] < 0$. In this Appendix, it will be shown that all of the eigenvalues of $e^{A_2 t_2} e^{A_1 t_1}$ are inside the unit circle for any $t_1, t_2 > 0$ under the spectral assumption above.

The stored energy in the circuit in stage S_1 or S_2 is given by the same formula, which involves capacitor voltages and inductor currents ($\frac{1}{2}\sum(L_i i_{Li}^2 + C_i v_{Ci}^2)$). Thus there exists a symmetric positive definite matrix $P \in \mathbf{R}^{N \times N}$ such that $A_1^T P + P A_1$ is negative semidefinite and, simultaneously, $A_2^T P + P A_2$ is negative definite.

Lemma A.1 *Let $A \in \mathbf{R}^{N\times N}$. Suppose $P \in \mathbf{R}^{N\times N}$ is symmetric positive definite. If $A^TP + PA$ is negative definite, then $e^{A^Tt}Pe^{At} - P$ is negative definite for any $t > 0$.*

Proof: Let $Q(t) = z^T(e^{A^Tt}Pe^{At} - P)z$, where $z \in \mathbf{R}^N$ is arbitrary. The function $Q(t)$ has the following properties:

$$\begin{aligned} \dot{Q}(t) &= z^Te^{A^Tt}(A^TP + PA)e^{At}z < 0 \\ Q(0) &= 0 \end{aligned}$$

Thus $Q(t) < 0$ for any $t > 0$ and the claim follows. □

The main result of this Appendix is

Proposition A.1 *Let the matrices A_1 and A_2 of the circuit model of Fig. 1 be such that* $\mathrm{Re}[\sigma(A_1)] \leq 0$ *and* $\mathrm{Re}[\sigma(A_2)] < 0$. *Then there exists a symmetric positive definite matrix $P \in \mathbf{R}^{N\times N}$ such that for any $t_1, t_2 > 0$.*

(i) $e^{A_1^Tt_1}Pe^{A_1t_1} - P$ *is negative semidefinite*

(ii) $e^{A_2^Tt_2}Pe^{A_2t_2} - P$ *is negative definite*

(iii) $\mathrm{Re}[\sigma(e^{A_2t_2}e^{A_1t_1})] < 0$

Proof:

Conclusions (i) and (ii) follow form the energy considerations discussed earlier in this Appendix, along with Lemma A.1. Now, note that

$$\begin{aligned} & e^{A_1^Tt_1}e^{A_2^Tt_2}Pe^{A_2t_2}e^{A_1t_1} - P \\ &= e^{A_1^Tt_1}e^{A_2^Tt_2}Pe^{A_2t_2}e^{A_1t_1} - e^{A_1^Tt_1}Pe^{A_1t_1} + e^{A_1^Tt_1}Pe^{A_1t_1} - P \\ &= e^{A_1^Tt_1}(e^{A_2^Tt_2}Pe^{A_2t_2} - P)e^{A_1t_1} + e^{A_1^Tt_1}Pe^{A_1t_1} - P \end{aligned}$$

which is negative definite. Thus, all of the eigenvalues of $e^{A_2t_2}e^{A_1t_1}$ lie strictly within the unit circle. □